Distribution of anthropogenic CO_2 in the Pacific Ocean

C. L. Sabine,[1] R. A. Feely,[2] R. M. Key,[3] J. L. Bullister,[2] F. J. Millero,[4] K. Lee,[5,6] T.-H. Peng,[5] B. Tilbrook,[7] T. Ono,[8] and C. S. Wong[9]

Received 14 September 2001; revised 11 April 2002; accepted 3 May 2002; published 14 November 2002.

[1] This work presents an estimate of anthropogenic CO_2 in the Pacific Ocean based on measurements from the WOCE/JGOFS/OACES global CO_2 survey. These estimates used a modified version of the ΔC^* technique. Modifications include a revised preformed alkalinity term, a correction for denitrification, and an evaluation of the disequilibrium terms using an optimum multiparameter analysis. The total anthropogenic CO_2 inventory over an area from 120°E to 70°W and 70°S to 65°N (excluding the South China Sea, the Yellow Sea, the Japan/East Sea, and the Sea of Okhotsk) was 44.5 ± 5 Pg C in 1994. Approximately 28 Pg C was located in the Southern Hemisphere and 16.5 Pg C was located north of the equator. The deepest penetration of anthropogenic CO_2 is found at about 50°S. The shallowest penetration is found just north of the equator. Very shallow anthropogenic CO_2 penetration is also generally observed in the high-latitude Southern Ocean. One exception to this is found in the far southwestern Pacific where there is evidence of anthropogenic CO_2 in the northward moving bottom waters. In the North Pacific a strong zonal gradient is observed in the anthropogenic CO_2 penetration depth with the deepest penetration in the western Pacific. The Pacific has the largest total inventory in all of the southern latitudes despite the fact that it generally has the lowest average inventory when normalized to a unit area. The lack of deep and bottom water formation in the North Pacific means that the North Pacific inventories are smaller than the North Atlantic. *INDEX TERMS:* 4806 Oceanography: Biological and Chemical: Carbon cycling; 4808 Oceanography: Biological and Chemical: Chemical tracers; 9355 Information Related to Geographic Region: Pacific Ocean; *KEYWORDS:* Pacific Ocean, anthropogenic CO_2, carbon cycle, total CO_2, delta C*, optimum multiparameter analysis

Citation: Sabine, C. L., R. A. Feely, R. M. Key, J. L. Bullister, F. J. Millero, K. Lee, T.-H. Peng, B. Tilbrook, T. Ono, and C. S. Wong, Distribution of anthropogenic CO_2 in the Pacific Ocean, *Global Biogeochem. Cycles*, *16*(4), 1083, doi:10.1029/2001GB001639, 2002.

1. Introduction

[2] Over the past 200 years, anthropogenic activities have led to a secular increase in atmospheric CO_2 from about 280 to greater than 365 ppmv [*Keeling and Whorf*, 2000; *Carbon Dioxide Information Analysis Center*, 2001]. The impact of this increase and that of other "greenhouse" gases on the global climate is at the center of a major international policy debate. Studies of the ocean's role in the uptake and storage of anthropogenic CO_2 and modulation of future atmospheric CO_2 levels are critical for understanding the global carbon cycle and for the prediction of future climate change.

[3] Data-based estimates of the current oceanic anthropogenic CO_2 inventories and transports have been greatly improved over the past decade by the global survey efforts of the World Ocean Circulation Experiment (WOCE), the Joint Global Ocean Flux Study (JGOFS), and the National Oceanic and Atmospheric Administration's (NOAA) Ocean Atmosphere Carbon Exchange Study (OACES). By working together, these programs have produced a large number of high-quality measurements of important anthropogenic tracers such as dissolved inorganic carbon (DIC), chlorofluorocarbons (CFCs), ^{13}C, and ^{14}C of DIC, as well as other chemical species important in the study of biogeochemical cycling. Data from these cruises are now becoming available and synthesis results are being published. A summary

[1]Joint Institute for the Study of Atmosphere and Ocean, University of Washington, Seattle, Washington, USA.
[2]NOAA/Pacific Marine Environmental Laboratory, Seattle, Washington, USA.
[3]AOS Program, Princeton University, Princeton, New Jersey, USA.
[4]University of Miami/RSMAS, Miami, Florida, USA.
[5]NOAA/Atlantic Oceanographic and Meteorological Laboratory, Miami, Florida, USA.
[6]Now at School of Environmental Science and Engineering, Pohang University of Science and Technology, Pohang, Republic of Korea.
[7]CSIRO, Division of Oceanography, Tasmania, Australia.
[8]Ecosystem Change Research Program, FRSGC/IGCR, Yokohama, Japan.
[9]Institute of Ocean Sciences, Sidney, British Columbia, Canada.

0886-6236/02/2001GB001639$12.00

of the objectives and accomplishments of the global CO_2 survey are given by *Wallace* [2001]. Carbon data from the Indian Ocean, for example, were used recently by *Sabine et al.* [1999] and *Goyet et al.* [1999] to estimate the anthropogenic CO_2 inventory in that ocean basin. *Sabine et al.*'s [1999] total anthropogenic CO_2 inventory estimates, based on the ΔC^* method of *Gruber et al.* [1996], showed that the deepest penetrations and highest column inventories of anthropogenic CO_2 are associated with the Subtropical Convergence with very little anthropogenic CO_2 in the high-latitude Southern Ocean (south of 50°S). *Gruber* [1998] found similar distributions in the South Atlantic based on pre-WOCE data. *Holfort et al.* [1998] used data from three WOCE/JGOFS sections together with several pre-WOCE cruises in the South Atlantic between 10°S and 30°S to estimate meridional carbon transports in this region. Notable findings by *Holfort et al.* [1998] are that the net preindustrial carbon transport across 20°S was toward the south, but the net anthropogenic CO_2 transport is toward the north. This results from the fact that the anthropogenic carbon is generally restricted to the upper, northward moving waters and the southward moving North Atlantic Deep Waters do not have a measurable anthropogenic CO_2 signal yet at this latitude.

[4] The Pacific Ocean is an important component in the global assessment of the oceanic uptake of anthropogenic CO_2. It accounts for nearly half of the total ocean volume and variability in the CO_2 fluxes from the equatorial Pacific associated with El Niño events may be responsible for up to one third of the interannual variability in atmospheric CO_2 growth rate [*Feely et al.*, 1999a]. Many studies have evaluated the uptake of anthropogenic CO_2 in the Pacific [e.g., *Chen*, 1982a, 1987; *Quay et al.*, 1992; *Chen*, 1993a, 1993b; *Tsunogai et al.*, 1993; *Slansky et al.*, 1997; *Ono et al.*, 1998; *Feely et al.*, 1999b; *Ono et al.*, 2000; *Watanabe et al.*, 2000; *Xu et al.*, 2000]. These studies, and others, suggest a wide range of uptake estimates for the North Pacific. The Pacific has been historically considered a small sink for anthropogenic CO_2 [e.g., *Chen*, 1982a]. However, some recent studies have suggested that the North Pacific is a larger sink than previously thought [e.g., *Tsunogai et al.*, 1993]. Most of these studies have focused on limited regions of the Pacific, relied on older data sets and techniques, or involved indirect approaches. This work uses the recently compiled CO_2 survey data from the Pacific to derive a basin-scale estimate of the Pacific anthropogenic CO_2 accumulated since preindustrial times.

2. The WOCE/JGOFS/OACES Data Set

[5] Between 1991 and 1996, carbon measurements were made on 26 cruises in the Pacific Ocean. This research was a collaborative effort between 15 laboratories and four countries (Table 1). Figure 1 shows the nearly 2000 station locations with carbon measurements in the Pacific. At least two carbon parameters were measured on almost all cruises, but the choice of which carbon pairs were measured varied between cruises. The quality of the carbon data was evaluated by *Lamb et al.* [2002]. A set of adjustments for certain cruises were recommended based on many lines of evidence including comparison of calibration techniques, results from Certified Reference Material (CRM) analyses, precision of at-sea replicate analyses, agreement between shipboard analyses and replicate shore-based analyses, comparison of deep water values at locations where two or more cruises overlapped or crossed, consistency with other hydrographic parameters, and internal consistency with multiple carbon parameter measurements. They estimated that the overall accuracy of the dissolved inorganic carbon (DIC) data after the recommended adjustments was $\sim$3 μmol kg^{-1}. Total alkalinity (TA), the second most common carbon parameter analyzed, had an overall accuracy of $\sim$5 μmol kg^{-1}. One should note that the *Lamb et al.* [2002] corrections were based on data sets that were first normalized to the certified CRM values. In cases where the reported data were not normalized, the adjustments noted in Table 1 include both the normalization factor and any additional corrections recommended by *Lamb et al.* [2002].

[6] TA is a required input for the ΔC^* calculation. The TA was calculated for all cruises where TA was not measured using DIC and fCO_2 or DIC and pH measurements together with the carbonate dissociation constants of *Merbach et al.* [1973] as refit by *Dickson and Millero* [1987] and ancillary constants listed in the program of E. Lewis and D. W. R. Wallace (Program developed for CO_2 system calculations, Oak Ridge National Laboratory, available at http://cdiac.esd.ornl.gov/oceans/, 1998). The final data set contained about 35,000 sample locations with DIC and TA values. This is over an order of magnitude more data than was available from the GEOSECS Pacific cruises ($\sim$2400 samples from 75 stations). The precision and accuracy is at least a factor of 2 better than GEOSECS [*Bradshaw et al.*, 1981; *Broecker et al.*, 1982]. A key factor in assuring the accuracy of the WOCE/JGOFS/OACES data set, which was not possible during GEOSECS, was the nearly universal analysis of CRM samples on the WOCE/JGOFS/OACES cruises (A. G. Dickson, Reference material batch information, Available at http://www-mpl.ucsd.edu/people/adickson/CO2_QC 2002) [*Dickson et al.*, 2002a, 2002b]. These samples provided a critical benchmark for comparing results from different laboratories on different cruises.

[7] The final version of the associated hydrographic and nutrient data for these cruises were generally downloaded from the WOCE program office. Data that were not finalized or available from the WOCE office were obtained from the PIs/chief scientists associated with the cruise. The quality of these data was recently evaluated by *Johnson et al.* [2001]. Overall, data quality was found to be within WOCE specs but small offsets could be detected for some parameters. Adjustments recommended by *Johnson et al.* [2001] were made to the data set used here, but these changes were generally too small to have a significant impact on the ΔC^* calculations (Table 1).

[8] The latest chlorofluorocarbon (CFC) data were compiled and evaluated by the U.S. WOCE CFC consortium. A synthesis of Pacific CFC data, led by J. Bullister, examined the overall quality of the data and ensured that all of the values were reported on the same concentration scale. Although no adjustments were made to the final reported CFC values, the revised data quality flags based on an

Table 1. Summary of Cruise Data Used in Anthropogenic CO_2 Analysis

Cruise Name	Cruise Date	Carbon Parameters Analyzed				Country Sponsor	Carbon Adjustments			Hydrographic Parameter Adjustment			
		DIC	TA	fCO_2	pH		DIC	TA	pH	NO_3	PO_4	$Si(OH)_4$	O_2
P8S	Jun-96	x	x		x	Japan	+2	+6	ND[a]	NA[b]	1.0391	1.0229	NA[b]
P9	Jul-94	x				Japan	+1.1	Calc.[c]	ND[a]	0.9831	NA[b]	NA[b]	NA[b]
P10	Oct-93	x	x			US	NA[b]	NA[b]	ND[a]	NA[b]	1.0260	NA[b]	NA[b]
P13	Aug-92	x	x			US	NA[b]	NA[b]	ND[a]	1.0327[d]	NA[b]	0.9804[d]	NA[b]
P14N	Jul-93	x	x		x	US	NA[b]	Calc.[e]	+0.0047	1.0115	1.0174	0.9800	NA[b]
P14S15S	Jan-96	x	x	x	x	US	NA[b]	Calc.[e]	+0.0047	NA[b]	NA[b]	NA[b]	NA[b]
P15N	Sep-94	x	x			Canada	−0.1	NA[b]	ND[a]	NA[b]	0.9821	NA[b]	NA[b]
EQS92	Mar-92	x	x	x	x	US	NA[b]	NA[b]	ND[a]	NA[b]	NO_3/16	NA[b]	NA[b]
P16C	Aug-91	x	x			US	NA[b]	NA[b]	ND[a]	NA[b]	NA[b]	NA[b]	NA[b]
P16N	Jan-91	x			x	US	+4	Calc.	+0.0047	NA[b]	NA[b]	NA[b]	NA[b]
P16S17S	Jul-91	x	x	x		US	+1.4	Calc.	ND[a]	NA[b]	0.9803	NA[b]	NA[b]
P16A17A	Oct-92	x		x		US	+1.3	Calc.	ND[a]	NA[b]	NA[b]	NA[b]	NA[b]
P17C	May-91	x	x			US	NA[b]	−9	ND[a]	1.0195	NA[b]	NA[b]	NA[b]
P17N	May-93	x	x			US	−7	−12	ND[a]	NA[b]	NA[b]	NA[b]	NA[b]
CGC91	Feb-91	x				US	NA[b]	Calc.[c]	ND[a]	NA[b]	NA[b]	NA[b]	NA[b]
P17E19S	Dec-92	x		x		US	+1.4	Calc.	ND[a]	NA[b]	0.9790	0.9814	NA[b]
P18S	Jan-94	x	x	x	x	US	NA[b]	Calc.[f]	+0.0047	1.0130	0.9722	NA[b]	NA[b]
P18N	Jan-94	x	x	x	x	US	NA[b]	Calc.[f]	ND[a]	1.0185	NA[b]	NA[b]	NA[b]
P19C	Feb-93	x		x		US	−0.2	NA[b]	ND[a]	NA[b]	0.9767	0.9860	NA[b]
P2	Jan-94	x	x		x	Japan	−4	+14	ND[a]	NA[b]	NA[b]	1.0171	NA[b]
P21E	Mar-94	x	x		x	US	NA[b]	NA[b]	+0.0047	NA[b]	NA[b]	NA[b]	1.0136
P21W	Mar-94	x	x		x	US	NA[b]	NA[b]	+0.0047	NA[b]	NA[b]	NA[b]	0.9703
P31	Jan-94	x	x		x	US	NA[b]	−6[e]	+0.0047	1.0150	NA[b]	NA[b]	NA[b]
P6	May-92	x		x		US	−0.6	Calc.	ND[a]	NA[b]	0.9813	NA[b]	NA[b]
S4P	Feb-92	x		x		US	−0.9	Calc.	ND[a]	1.0241	0.9715	0.9810	NA[b]
SR3S4	Dec-94	x	x			Australia	NA[b]	NA[b]	ND[a]	NA[b]	NA[b]	NA[b]	NA[b]

[a] ND = no data.
[b] NA = no adjustment recommended.
[c] Values estimated from MLR using hydrographic parameters from nearby stations with measured TA.
[d] Leg 2 stations adjusted only (>5°S).
[e] Calculated only where TA missing using DIC/pH.
[f] Calculated only where TA missing using DIC/fCO_2.

analysis of all the cruises provided a much cleaner data set for the ΔC* calculations.

3. Approach

[9] The first anthropogenic CO_2 estimates calculated from DIC and TA measurements were presented over 20 years ago by *Brewer* [1978] and *Chen and Millero* [1979]. The basic approach assumes that the anthropogenic signal can be isolated from the measured DIC by subtracting off the changes due to biology and a preindustrial, preformed DIC concentration. Variations of the original Brewer and Chen/Millero approach have been used to estimate anthropogenic CO_2 in many regions of the world [e.g., *Chen*, 1982a, 1982b; *Papaud and Poisson*, 1986; *Poisson and Chen*, 1987; *Krumgalz et al.*, 1990; *Brewer et al.*, 1997; *Körtzinger et al.*, 1999]. However, this approach has not found general acceptance, since the assumptions led to uncertainties that were generally regarded as too large [*Shiller*, 1981; *Broecker et al.*, 1985; *Wanninkhof et al.*, 1999; *Sabine and Feely*, 2001].

[10] *Gruber et al.* [1996], building on the work of Brewer and Chen/Millero, developed the ΔC* technique for estimating anthropogenic CO_2 to resolve many of the uncertainties associated with the original approach. The most significant improvement was that rather than trying to empirically derive a preformed DIC concentration, *Gruber et al.* [1996] calculated the DIC concentration the waters would have in equilibrium with a preindustrial atmosphere based on the thermodynamics of the carbon system. Because CO_2 gas exchange is relatively slow [*Broecker and Peng*, 1974], an additional term was added to account for the fact that surface waters are rarely in complete equilibrium with the atmosphere. The basic approach can be summarized with the following simple equation:

$$C_{anth} = C_m - \Delta C_{bio} - C_{280} - \Delta C_{diseq}, \quad (1)$$

where

C_{anth} = anthropogenic carbon concentration in μmol kg^{-1};
C_m = measured DIC concentration in μmol kg^{-1};
ΔC_{bio} = DIC (μmol kg^{-1}) changes resulting from the remineralization of organic matter and the dissolution of calcium carbonate particles;
C_{280} = DIC (μmol kg^{-1}) of waters in equilibrium with an atmospheric CO_2 of 280 μatm;
ΔC_{diseq} = air-sea CO_2 difference (i.e., ΔfCO_2) expressed in terms of DIC (μmol kg^{-1}).

The first three terms on the right-hand side of equation (1) make up the quasiconservative ΔC* tracer. These terms can be determined explicitly for every water sample as discussed in section 3.1. The ΔC_{bio} and C_{280} terms generally account for more than 95% of the measured DIC concentration. The small remaining ΔC_{diseq} term

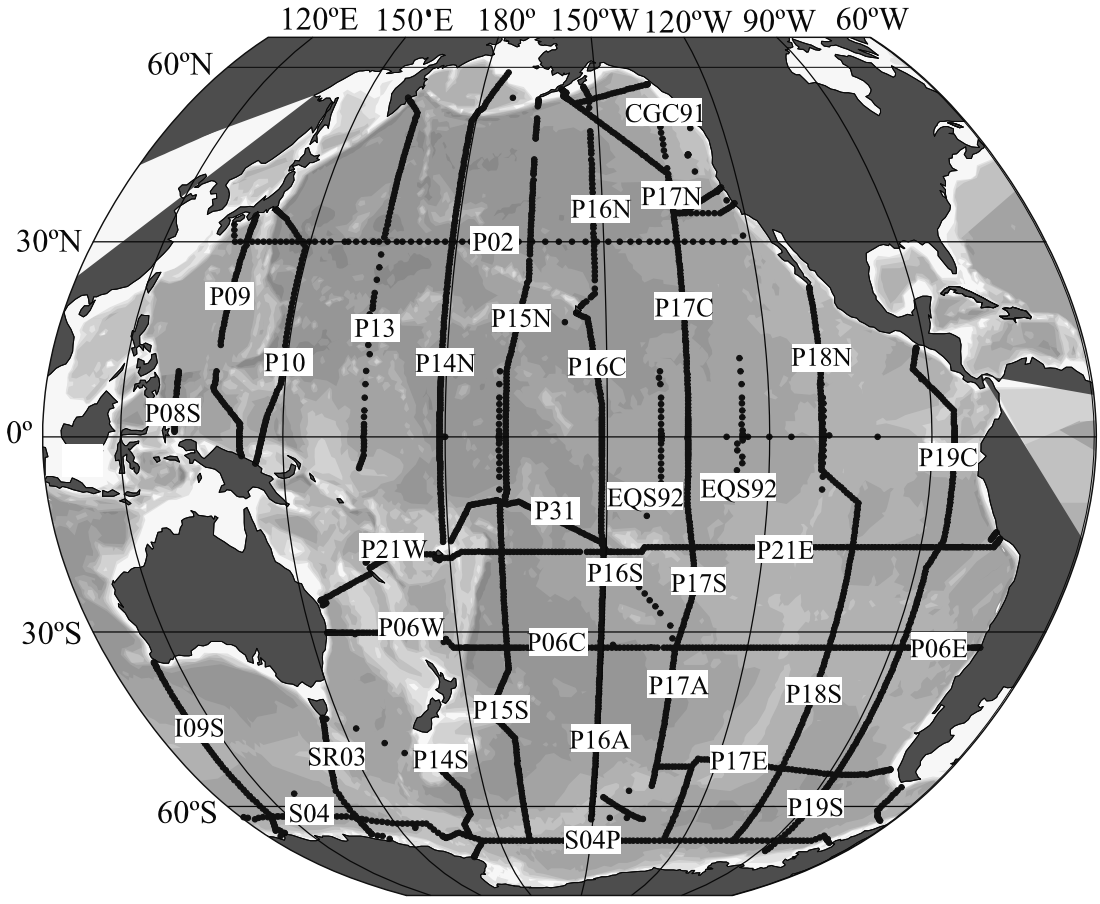

Figure 1. Map of station locations from the WOCE/JGOFS/OACES Pacific survey using a Mollweide projection.

requires the use of a water mass age tracer to evaluate as discussed in section 3.2.

3.1. Calculation of ΔC*

[11] The quasiconservative tracer, ΔC*, is defined as the difference between the measured DIC concentration, corrected for biology and the DIC concentration these waters would have at the surface in equilibrium with a preindustrial atmosphere (i.e., $\Delta C^* = C_m - \Delta C_{bio} - C_{280}$). The biological correction has two components. The organic component uses changes in AOU, together with a stoichiometric C:O ratio, to estimate how much DIC has increased due to organic remineralization since leaving the surface. The second component uses the difference between the measured TA and a preformed TA (TA°) to estimate the changes in DIC resulting from the dissolution of calcium carbonate particles. There is also a small organic adjustment on the carbonate correction term to account for the effect of the proton flux on TA. The stoichiometric ratios used for the biological corrections are based on the work of *Anderson and Sarmiento* [1994]. The C_{280} term uses a linearized form of the carbonate equilibrium equations [A2 from *Gruber et al.*, 1996] together with the preformed alkalinity and an fCO_2 value of 280 μatm to calculate the equilibrium DIC concentration.

[12] The ΔC* calculation used for this study is essentially the same as that originally defined by *Gruber et al.* [1996] with two small differences: a modification of the preformed alkalinity term, TA°, based on the new global survey data and the addition of a denitrification term in the biological correction,

$$\begin{aligned}\Delta C^* = {} & C_m - C_{280} + 117/170(O - O_{sat}) \\ & - 1/2(TA - TA^\circ - 16/170(O - O_{sat})) \\ & + 106/104N^*_{anom}, \end{aligned} \quad (2)$$

where TA and O are the measured concentrations for a given water sample in μmol kg^{-1}, O_{sat} is the calculated oxygen saturation value that the waters would have at their potential temperature and one atmosphere total pressure (i.e., if they were adiabatically raised to the surface), and N^*_{anom} is the N* anomaly described later in this section.

[13] The TA° formulation of *Gruber et al.* [1996] was based on a multiple linear regression fit of surface TA values from the GEOSECS, SAVE, and TTO cruises. *Sabine et al.* [1999] derived a revised TA° equation based on the WOCE/JGOFS Indian Ocean data. The TA° term was re-examined here with respect to the Pacific data set. Neither the *Sabine et al.* [1999] nor the *Gruber et al.* [1996] equations were

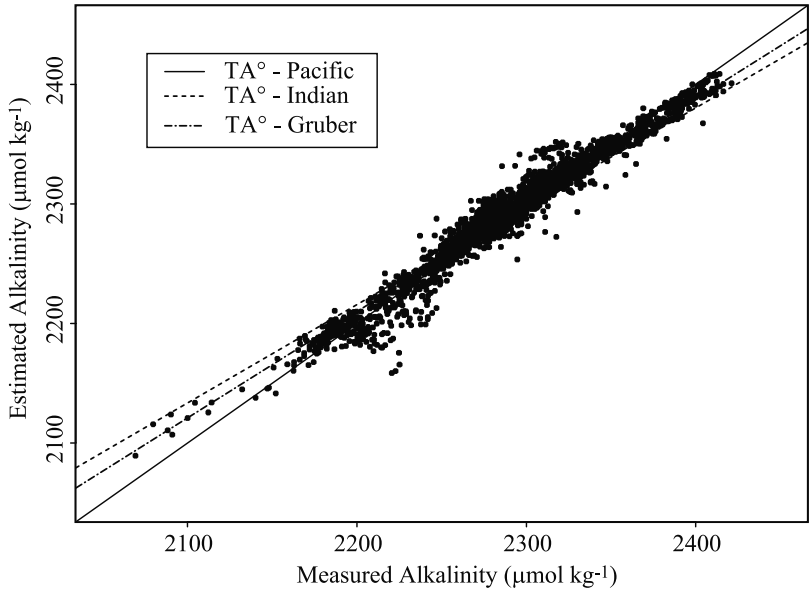

Figure 2. Plot of surface alkalinity (pressure <60 dbar) estimated from temperature, salinity, and PO versus measured alkalinity from the Pacific survey. Solid line and points show results from a fit of the Pacific data (Equation 3). Dashed line is based on *Sabine et al.* [1999] equation from the Indian Ocean. Dash-dotted line is based on *Gruber et al.* [1996] equation.

found to fit the shallow Pacific data perfectly (Figure 2). Both equations overestimated the alkalinity at low values and underestimated at higher values. A new equation was derived using all of the Pacific alkalinity data shallower than 60 m (~1900 data points). The form of the equation is the same as that used by *Sabine et al.* [1999],

$$TA^\circ = 148.7[\pm 9] + 61.36[\pm 0.3]S + 0.0941[\pm 0.005]PO - 0.582[\pm 0.07]\theta, \quad (3)$$

where S is salinity, PO is a quasiconservative tracer similar to that introduced by *Broecker* [1974] (PO = dissolved oxygen + 170*phosphate), and θ is the potential temperature. The standard error in the Pacific TA° equation is ±9 μmol kg^{-1}. A standard ANOVA analysis of the fit shows that all four terms are highly significant.

[14] *Sabine et al.* [1999] also proposed a correction to the biological adjustment in equation (1) to account for denitrification in the water column. Denitrification remineralizes carbon with a very different stoichiometric ratio to nitrogen than standard aerobic respiration [*Anderson*, 1995; *Gruber and Sarmiento*, 1997],

$$C_{106}H_{175}O_{42}N_{16}P + 150O_2 = 106CO_2 + 16HNO_3 + H_3PO_4 + 78H_2O \quad (4)$$

$$C_{106}H_{175}O_{42}N_{16}P + 104NO_3^- = 4CO_2 + 102HCO_3^- + 60N_2 + HPO_4^{2-} + 36H_2O. \quad (5)$$

Sabine et al. [1999] estimated the denitrification signal using the N* tracer of *Gruber and Sarmiento* [1997]. A slightly more generalized version of this equation has since been proposed by *Deutsch et al.* [2001],

$$N^* = N - 16P + 2.90. \quad (6)$$

The only change from the *Gruber and Sarmiento* [1997] equation was that the original equation was scaled by a factor of 0.87. The revised equation is simpler and is more general because it removes built in assumptions about the nitrogen loss from the organic reservoir [*Deutsch et al.*, 2001]. In practice, this modification actually has no impact on the final denitrification corrections since that signal is identified as an N* anomaly from the mean. The mean N* value for this data set was -1.5 μmol kg^{-1}, in agreement with the findings of *Deutsch et al.* [2001]. The denitrification stoichiometric ratio of 106/104 from equation (5) [*Gruber and Sarmiento*, 1997] was used to correct the ΔC* values in equation (2) where N* showed a negative anomaly. The distribution of the anomalies (i.e., in the eastern Tropical Pacific and to a lesser extent in the western subtropical North Pacific) also agrees with *Deutsch et al.* [2001] and is discussed in detail in that work.

3.2. Estimation of ΔC_{diseq}

[15] Rearrangement of equation (1) shows that ΔC* reflects both the anthropogenic signal and the preserved air-sea CO_2 difference expressed in terms of DIC (i.e., $\Delta C^* = C_{anth} + \Delta C_{diseq}$). For given isopycnal surfaces, the air-sea disequilibrium component can be discriminated from the anthropogenic signal using either information about the water age (e.g., from transient tracers such as CFCs or ^3H-^3He) or the distribution of ΔC* in regions not affected by the anthropogenic transient. In the case where C_{anth} can be assumed to be zero over some portion of an isopycnal surface (i.e., $\Delta C^* = 0 + \Delta C_{diseq}$), the disequilibrium term is set equal to the average of the ΔC* values for that portion of the surface. For shallow surfaces, that cannot be assumed to be free of anthropogenic CO_2, we use the ΔC^*_t term of *Gruber et al.* [1996]. ΔC^*_t is derived in the same manner as

ΔC^*, but rather than evaluating the carbon concentration the waters would have in equilibrium with a preindustrial atmosphere, they are evaluated with respect to the CO_2 concentration the atmosphere had when the waters were last at the surface based, in this study, on the concentration ages determined from CFC-12 measurements (ΔC^*_{t12}),

$$\Delta C^*_{t12} = C_m - C_{teq} + 117/170(O - O_{sat}) - 1/2(TA - TA^\circ - 16/170(O - O_{sat})) + 106/104N^*_{anom}, \quad (7)$$

where C_{teq} is DIC calculated from TA° and the atmospheric fCO_2 value at the time the waters were last at the surface (date of sample collection minus CFC age). The ΔC_{diseq} terms for these surfaces are then set equal to the mean of the ΔC^*_{t12} values on each surface.

[16] Several papers have been published recently evaluating the ΔC^* approach for estimating anthropogenic CO_2 [e.g., *Wanninkhof et al.*, 1999; *Coatanoan et al.*, 2001; *Sabine and Feely*, 2001; *Orr et al.*, 2001]. It has been recognized that the evaluation of the ΔC_{diseq} term is one of the most problematic steps in the estimation of anthropogenic CO_2. One important assumption in the evaluation of ΔC_{diseq} is that the global mean air-sea CO_2 disequilibrium has remained constant over time. Although this assumption is consistent with most contemporary CO_2 time-series measurements in the Pacific [e.g., *Inoue et al.*, 1995; *Winn et al.*, 1998; *Feely et al.*, 1999a; *Takahashi et al.*, 1999], it cannot be true over timescales extending into the preindustrial period or the oceans would not be acting as a sink for anthropogenic CO_2. *Gruber et al.* [1996] estimated that an average global uptake of about 2 Pg C yr^{-1} would correspond to an air-sea disequilibrium of about 5 μmol kg^{-1} in ΔC_{diseq}. If this signal is spread out over the entire record since preindustrial times it would be very difficult to see in ΔC^* given the uncertainties in the calculation. This 5 μmol kg^{-1} uncertainty can be considered the theoretical minimum detection limit for this technique as it is currently used.

[17] Another difficulty with the evaluation of the ΔC_{diseq} term is the proper characterization of mixing. In the past, the ΔC_{diseq} term has been evaluated on isopycnal surfaces assuming either no mixing or simple two end member mixing along the isopycnal [*Gruber et al.*, 1996; *Gruber*, 1998; *Sabine et al.*, 1999]. This work attempts to improve upon this approach by using the Optimum Multiparameter (OMP) analysis to explicitly solve for the mixing terms. The multiparameter analysis was introduced by *Tomczak* [1981] by adding oxygen and nutrients as additional quasi-conservative parameters, assuming that biogeochemical changes were negligible. The OMP technique evolved over the next two decades to account for the nonconservative behavior of biological parameters using stoichiometric ratios, allowing for improved determinations of mixing coefficients for multiple water-types [e.g., *Tomczak and Large*, 1989; *You and Tomczak*, 1993; *Karstensen and Tomczak*, 1998; *Pérez et al.*, 2001].

[18] The OMP analysis used here determines the best linear mixing combination in parameter space of temperature (T), salinity (S), oxygen (O), phosphate (P), nitrate (N), and silicate (Si) by minimizing the residuals (R) of the following equations in a least squares sense:

$$x_1T_1 + x_2T_2 + x_3T_3 + x_4T_4 + x_5T_5 = T_{obs} + R_T, \quad (8)$$

$$x_1S_1 + x_2S_2 + x_3S_3 + x_4S_4 + x_5S_5 = S_{obs} + R_S, \quad (9)$$

$$x_1P_1 + x_2P_2 + x_3P_3 + x_4P_4, + x_5P_5 + \Delta P = P_{obs} + R_P \quad (10)$$

$$x_1O_1 + x_2O_2 + x_3O_3 + x_4O_4, + x_5O_5 - r_{O/P}\Delta P = O_{obs} + R_O \quad (11)$$

$$x_1N_1 + x_2N_2 + x_3N_3 + x_4N_4, + x_5N_5 + r_{N/P}\Delta P = N_{obs} + R_N \quad (12)$$

$$x_1Si_1 + x_2Si_2 + x_3Si_3 + x_4Si_4, + x_5Si_5 + r_{Si/P}\Delta P = Si_{obs} + R_{Si} \quad (13)$$

$$x_1 + x_2 + x_3 + x_4 + x_5 = 1 + R_\Sigma, \quad (14)$$

where x_i is the water mass fraction for up to five water types. The measured properties are denoted by the subscript "obs," while the end member concentrations are denoted by numbers. ΔP is the estimated change in phosphate due to biological production/remineralization. The phosphate change is related to the change in other bioactive tracers using the stoichiometric ratios (r) of *Anderson and Sarmiento* [1994]. This set of seven equations with six unknowns is solved for each sample location. The impact of any one parameter on the final mixing fraction is determined by a weighting function that is based on the estimated accuracy and the dynamic range of the measurements. The OMP routines are available on the World Wide Web from J. Karstensen and M. Tomczak (http://www.ldeo.columbia.edu/~jkarsten/omp_std/, 2002).

[19] The OMP analysis was performed on four blocks of data based on potential density (σ_θ). The first block included data from the main thermocline ($25.9 > \sigma_\theta \geq 26.9$), where measurable CFCs are present throughout the surface. Five source water types were identified for these data based on descriptions of water masses in the literature [e.g., *Reid*, 1997] and from examination of the temperature-salinity (T-S) properties of the data (Table 2). The end member properties were determined by taking the mean and standard deviation of the mean for roughly 40–50 points defining the extremes of temperature, salinity, or oxygen with respect to the disequilibrium values (Figure 3). The nonconservative component of the biological parameters was derived using the same stoichiometric ratios used for the ΔC^* calculations [i.e., *Anderson and Sarmiento*, 1994]. The biological parameters were discounted in the OMP weighting function to minimize the potential errors introduced by using imperfect stoichiometric ratios. Weighting for the mass conservation equation, conservative parameters, and biological parameters were given as 48, 24, and 2, respectively. A discussion of the error analysis is given in the next section.

[20] The objective of this exercise was to derive the net disequilibrium values of the mixed waters, so emphasis was placed on identifying those water types with unique disequilibrium signals. The disequilibrium values for all of the water types in the first density interval were derived from the ΔC^*_{t12} calculation (7). The ΔC_{diseq} value for each water type was determined from the mean ΔC^*_{t12} values where the CFC-12

Table 2. Water Type Properties Used in OMP Analysis

ID	Latitude	Theta, °C	STDM Theta	Salinity	STDM Salanity	Oxygen µmol kg^{-1}	STDM Oxygen,	PO_4, µmol kg^{-1}	STDM PO_4	NO_3, µmol kg^{-1}	STDM NO_3	$Si(OH)_4$, µmol kg^{-1}	STDM $Si(OH)_4$	Diseq µmol kg^{-1}	STDM Diseq.	Approach
1a	1°N	12.87	0.20	34.880	0.010	46.40	5.0	2.023	0.040	28.55	0.60	23.11	0.70	5.89	0.30	ΔC^*_{t12}
1b	25°S	16.24	0.07	35.450	0.010	191.50	2.0	0.055	0.020	6.32	0.30	2.30	0.07	−10.38	0.70	ΔC^*_{t12}
1c	50°N	3.24	0.10	33.580	0.020	166.60	8.0	2.480	0.040	33.98	0.60	71.33	2.00	−4.85	1.00	ΔC^*_{t12}
1d	48°S	8.37	0.10	34.550	0.020	267.80	1.0	1.120	0.020	15.37	0.30	4.73	0.10	−4.03	0.40	ΔC^*_{t12}
1e	44°N	7.19	0.30	33.470	0.030	215.70	4.0	1.560	0.060	19.97	0.80	27.72	2.00	−6.24	0.90	ΔC^*_{t12}
2a	50°N	3.60	0.03	33.890	0.005	62.10	2.0	2.890	0.020	41.17	0.20	92.88	0.70	−9.84	1.00	ΔC^*_{t12}
2b	3°S	8.41	0.03	34.650	0.002	34.16	5.0	2.580	0.040	37.71	0.50	39.18	1.00	8.86	0.60	ΔC^*
2c	4°N	3.71	0.02	34.580	0.001	73.17	3.0	2.930	0.020	40.91	0.30	106.25	0.80	−4.57	0.60	ΔC^*
2d	60°S	1.32	0.10	34.000	0.006	314.37	1.0	1.900	0.010	27.60	0.20	22.56	1.00	−15.27	0.80	ΔC^*_{t12}
2e	54°S	5.31	0.04	34.220	0.002	282.57	1.0	1.540	0.010	22.11	0.20	9.42	0.20	−7.40	0.60	ΔC^*_{t12}
3a	56°S	1.96	0.01	34.710	0.001	181.84	0.4	2.200	0.009	32.01	0.05	84.69	0.80	−11.42	0.40	ΔC^*
3b	67°S	0.13	0.20	34.340	0.007	263.35	7.0	2.160	0.020	31.66	0.40	70.94	0.90	5.56	1.00	ΔC^*
3c	45°N	2.37	0.01	34.470	0.002	30.47	0.9	3.050	0.010	43.17	0.10	157.78	0.70	−2.52	0.80	ΔC^*
3d	4°S	3.38	0.01	34.580	0.002	83.06	3.0	2.890	0.020	40.49	0.30	107.33	1.00	−4.94	0.50	ΔC^*
4a	56°S	1.85	0.01	34.740	0.001	190.41	0.3	2.140	0.004	31.04	0.07	83.66	0.60	−14.13	0.20	ΔC^*
4b	67°S	−0.22	0.10	34.600	0.007	244.59	6.0	2.170	0.010	31.58	0.17	87.83	1.00	−7.80	0.80	ΔC^*
4c	43°N	1.33	0.01	34.670	0.001	110.85	2.0	2.770	0.030	38.24	0.08	191.52	4.00	−8.73	0.70	ΔC^*
4d	67°S	−0.26	0.02	34.700	0.001	230.40	0.9	2.180	0.004	32.01	0.07	107.15	1.00	−12.46	0.20	ΔC^*

STDM = standard deviation of the mean.

age was less than 30 years in the same sample groupings as the end member properties used in the OMP analysis (Figure 3). The net disequilibrium value for each of the observations ($\Delta C_{diseqobs}$) was determined from the OMP derived mixing fractions and the disequilibrium values for the different water types ($\Delta C_{diseq\ i}$),

$$\Delta C_{diseqobs} = \sum_{i=1}^{i=5} x_i \Delta C_{diseq\ i}. \quad (15)$$

[21] One of the more difficult regions for determining ΔC_{diseq} is in the intermediate waters where low CFC concentrations make the water mass ages less reliable, yet the assumption that portions of the surface are free of anthropogenic CO_2 make the ΔC^* approach problematic. The OMP analysis helps alleviate some of the difficulties in this region because different water types can be defined using different procedures. The second data block analyzed with the OMP ($26.9 > \sigma_\theta \geq 27.5$) contained some water types, such as the high-latitude intermediate and mode waters, which had enough CFCs to determine ΔC^*_{t12} based ΔC_{diseq} values. Other water types, such as the tropical end members, were well removed from the measurable CFCs so the ΔC^* approach could be used to determine the ΔC_{diseq} values (Table 2). The mixture of these different water types at intermediate latitudes can be determined from the OMP in a manner that was not possible with the techniques used in the previous ΔC^* approaches. The result is a smoother transition from one approach to the other and resulting disequilibrium estimates that are more oceanographically consistent.

[22] The final two data blocks analyzed with the OMP ($27.5 > \sigma_\theta \geq 27.75$ and $\sigma_\theta > 27.75$) characterize the deep Pacific. Fewer water types were required to describe these data and the ΔC_{diseq} values could be determined using the mean ΔC^* values for waters that were free of CFCs. The small high-latitude Southern Ocean regions that had deep waters with CFC ages less than 30 years were handled in the same manner as samples in the upper 150 m, by taking the observed ΔC^*_{t12} values calculated for each individual sample as the ΔC_{diseq}. Once all of the ΔC_{diseq} values were determined, anthropogenic CO_2 concentrations were calculated as the difference between ΔC^* and ΔC_{diseq}.

4. Evaluation of Errors

[23] Error evaluation for the ΔC^* method is difficult because of potential systematic errors associated with some of the parameters (i.e., the biological correction). The random errors should not significantly affect the inventory estimates determined here; however, systematic errors can potentially bias the estimated inventories and are handled separately.

4.1. ΔC^* Calculations

[24] The random errors associated with the anthropogenic CO_2 estimates can be determined by propagating through the precision of the various measurements required for the calculation as demonstrated by *Sabine et al.* [1999]. The terms involving the C:O are evaluated separately below because the random errors cannot be isolated from potential

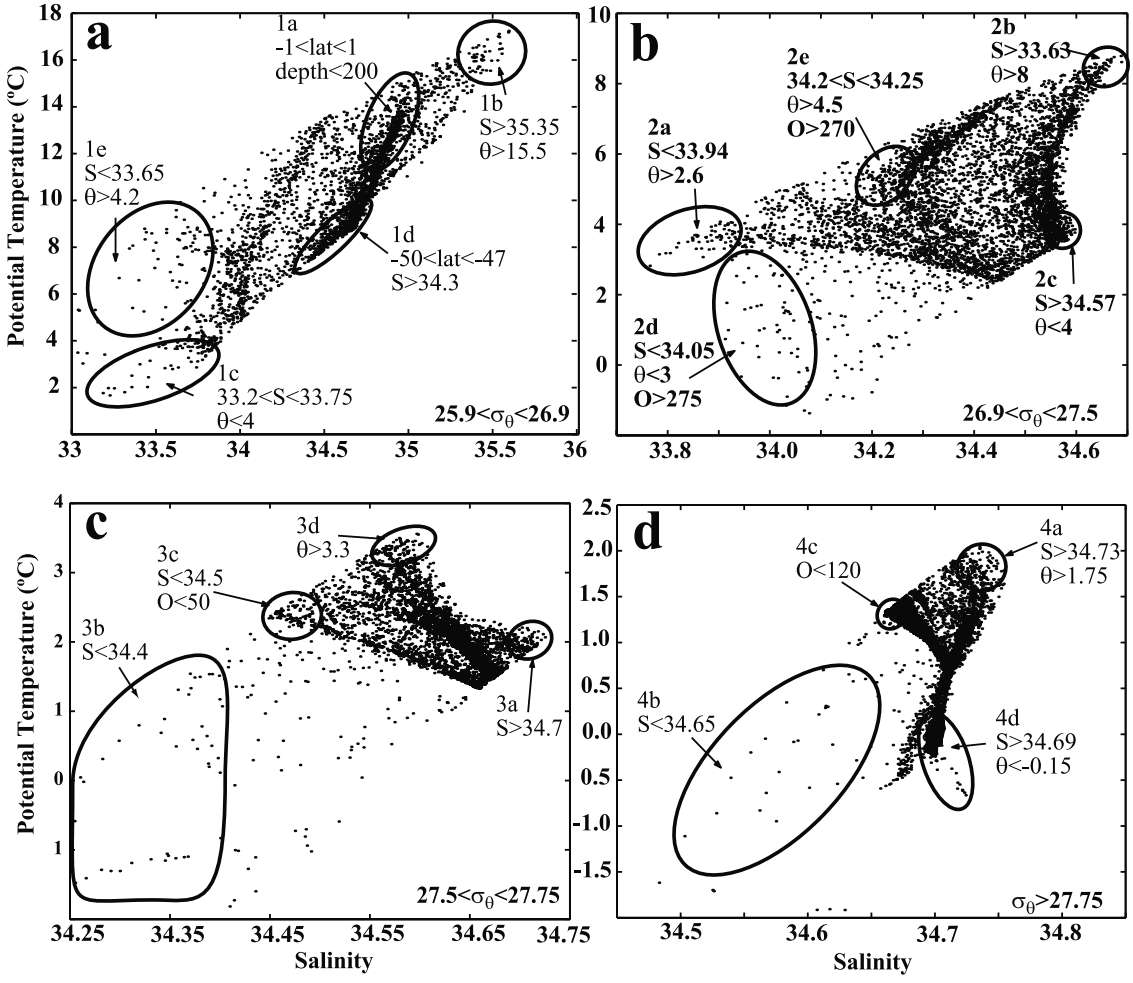

Figure 3. Temperature-salinity diagrams for all Pacific data points with carbon measurements. The four panels show the data from the four OMP analyses. The large ovals and text indicate the data used and selection criteria for determining the water types (O = dissolved oxygen in μmol kg^{-1}; S = salinity; θ = potential temperature in °C; lat = degrees of latitude with negative values indicating Southern Hemisphere; depth is in meters).

systematic errors. The individual error estimate for each term used in this calculation was either taken from the appropriate WOCE cruise reports, from *Lamb et al.* [2002], or from previously determined estimates given by *Sabine et al.* [1999]. The primary difference between the technique used in the Indian Ocean and this work is in the determination of the ΔC_{diseq}. The error evaluation should include estimated errors in both the end member water types and the mixing ratios derived from the OMP analysis.

[25] The OMP mixing ratios were evaluated using a set of Monte Carlo simulations where each of the end member water properties were randomly varied about their mean values 1000 times and run through the OMP routines. The variation of each property was based on a two-sigma estimate of the standard deviation of the mean for each water type (Table 2). The resulting 1000 mixing ratio estimates are multiplied by the mean ΔC^*_{t12} or ΔC^* terms for each water type to give estimates of the net ΔC_{diseq} values for each data point. The error in the mixing terms (σ_J) is given by the average standard deviation of the resulting net ΔC_{diseq} estimates. The largest errors in the mixing terms (±1.87 μmol kg^{-1}) were observed in the shallow OMP analysis group where water properties are most variable. The errors in the intermediate (±0.52 μmol kg^{-1}) and deep waters (±0.065 μmol kg^{-1}) were much smaller.

[26] In a similar manner, the errors associated with the estimation of the end member disequilibrium values were evaluated by randomly varying the mean end member ΔC^*_{t12} or ΔC^* terms 1000 times based on a two-sigma estimate of the standard deviation of the mean for each water type (Table 2). These values were then multiplied by the mean mixing ratios estimated for each data point. The error in the end member disequilibrium ($\sigma_{\Delta Cdiseq\ J}$) is given by the average standard deviation for the resulting net ΔC_{diseq} estimates. The surface water disequilibrium errors (±0.42 μmol kg^{-1}) were only about 20% of the errors from the mixing ratios. This trend is reversed in the deep waters where the mixing errors are much smaller, but the disequilibrium errors are about the same as in the surface (±0.40

μmol kg^{-1}). The smallest errors associated with the end member disequilibrium terms ($\pm$0.09 μmol kg^{-1}) are found in the intermediate waters.

[27] The errors associated with both the mixing coefficients and the end member disequilibrium values appear to be much smaller than the random errors associated with other parts of the ΔC^* calculation. Propagating all of these errors together results in an overall estimated error of 7.5 μmol kg^{-1}. This estimate is larger than the standard deviation of the ΔC^* values below the deepest anthropogenic CO_2 penetration depth ($\pm$3.6 μmol kg^{-1} for pressure >2000 dbar and latitudes north of 50°S) suggesting that the propagated errors may be an overestimate of the random variability. Taking a mean value between these two estimates and considering the minimum theoretical uncertainty discussed in section 3.2, we estimate the minimum detection level for these estimates to be about $\pm$5 μmol kg^{-1}.

[28] The potential systematic errors associated with the anthropogenic CO_2 calculation are much more difficult to evaluate. The random error estimate above includes all terms except those associated with the C:O biological correction. Although other terms involving N:O and N:P corrections potentially have systematic offsets associated with errors in the ratio estimates, the only potentially significant errors involve the C:O corrections [*Gruber et al.*, 1996; *Gruber*, 1998]. The validity of the *Anderson and Sarmiento* [1994] stoichiometric ratios has been discussed by *Gruber et al.* [1996], *Gruber* [1998], and *Sabine et al.* [1999]. Although several investigators have found evidence of variable stoichiometric ratios [e.g., *Sambrotto et al.*, 1993], the ΔC^* calculations consistently indicate that the *Anderson and Sarmiento* [1994] ratios provide the most reliable results [e.g., see *Sabine et al.*, 1999, Figure 6]. The range of stoichiometric ratios published in the literature may reflect differences in timescale for the observations. The *Anderson and Sarmiento* [1994] approach used water chemistry data that integrated over relatively long timescales. In this respect, the *Anderson and Sarmiento* [1994] approach is the most consistent with the techniques used for the ΔC^* calculations.

[29] A sensitivity study was used to evaluate the potential error associated with variable C:O values. Two additional estimates of anthropogenic CO_2 were determined by taking the low and high C:O values (-0.60 and -0.78) given by the error estimates of *Anderson and Sarmiento* [1994]. Since the C:O correction applies to both ΔC^* and the ΔC^*_{t12} terms, the disequilibrium values were reevaluated in the same manner as described above. The total range of anthropogenic values from these three estimates varied as a function of apparent oxygen utilization (AOU) from -23 to 26 with an average difference in the upper 1000 m of only 1.3 ± 5 and -1.4 ± 5 μmol kg^{-1} for the -0.60 and -0.78 cases, respectively. Because the C:O correction affects both the ΔC^* and ΔC_{diseq} terms together, much of the systematic error in the final anthropogenic estimate ($\Delta C^* - \Delta C_{diseq}$) cancels out (see equations (2) and (7)). They do not completely cancel out because the ΔC^* values are derived for each sample location whereas the ΔC_{diseq} term is an average from a number of observations at a similar density. The average errors estimated from the sensitivity study are much smaller than the estimated uncertainty of the random errors estimated above, but are likely to contribute much more significantly to the overall inventory estimates.

4.2. Inventory Estimates

[30] Basin-wide anthropogenic concentrations were evaluated on a 1° grid at 42 levels with intervals ranging from 25 m near the surface to 200 m below 2800 m using the objective mapping techniques of *Sarmiento et al.* [1982]. Total anthropogenic CO_2 was mapped over an area from 120°E to 70°W and 70°S to 65°N (excluding areas of land, the South China Sea, the Yellow Sea, the Japan/East Sea, and the Sea of Okhotsk). The values at each level were multiplied by the volume of water in each slab and summed to generate the total anthropogenic CO_2 inventory. The method of integrating mapped surfaces compared very well with the technique of vertically integrating each station and mapping the station integrals.

[31] It is extremely difficult to evaluate a reasonable estimate of the potential errors associated with the inventory estimates [*Goyet and Davis*, 1997]. A simple propagation of errors implies that the random errors associated with any individual anthropogenic estimate is approximately $\pm$7.5 μmol kg^{-1}, but these errors should essentially cancel out for an integrated inventory based on nearly 35,000 individual estimates. Systematic errors have by far the largest impact on the inventory estimates. Sensitivity studies with the C:O variations give a range of total inventory estimates of $\pm$5 Pg C. Other systematic errors could also be generated from the denitrification term, the terms involving N:O, and the time differences for the various cruises. The magnitude of these errors is believed to be much smaller than the uncertainty in the C:O correction. Because the survey cruises were run with very close station spacing along the track, but often 20 or more degrees of longitude/latitude between lines, the potential also exists for large mapping errors. Because of the zonal nature of the Pacific, however, we believe these errors are not large. We feel that the sensitivity studies represent a reasonable estimate of the overall uncertainty of the total inventory. An error of roughly 10–15% of the total inventory (i.e., 44.5 $\pm$ 5 Pg C) is comparable to previous error estimates using this technique [*Gruber et al.*, 1996; *Gruber*, 1998; *Sabine et al.*, 1999]. Errors for regional inventories are assumed to scale to the total.

5. Results

[32] Anthropogenic CO_2 concentrations in the Pacific reach a maximum value of about 50 μmol kg^{-1}. The highest concentrations (typically 40–45 μmol kg^{-1}) are found in the subtropical surface waters. These surface concentrations are slightly lower than expected values based on thermodynamic considerations and the observed atmospheric CO_2 history. The distribution of anthropogenic CO_2 in the ocean interior (along WOCE section P16 at ~150°W) is similar to the distribution of other anthropogenic tracers in the central Pacific (Figure 4). The deepest penetration of anthropogenic CO_2 is found at about 50°S associated with the Subtropical Convergence. The shallowest penetrations are observed in

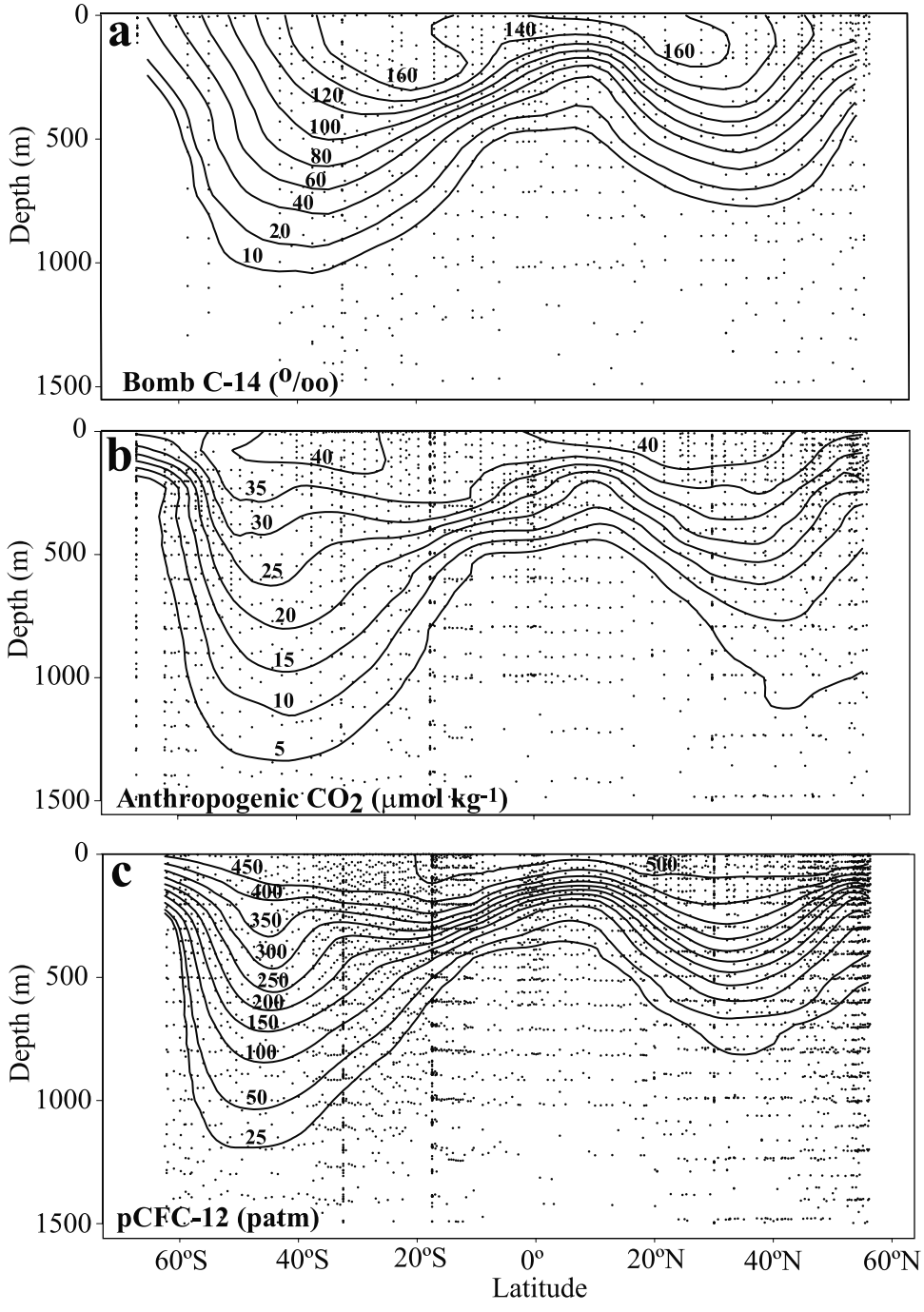

Figure 4. (a) Meridional sections of bomb C-14 in ‰ (b) anthropogenic CO_2 in μmol kg^{-1}, and (c) pCFC-12 in patm along 150°W in the central Pacific. Points indicate sample locations. Bomb C-14 calculated from data provided by R. Key (Princeton) using the potential alkalinity method of *Rubin and Key* [2002]. The pCFC-12 calculated using data from J. Bullister (NOAA/PMEL).

the high-latitude Southern Ocean and just north of the equator associated with a doming of the isopycnals between the westward moving North Equatorial Current and the eastward moving North Equatorial Countercurrent. The general structure of the anthropogenic CO_2 in the Pacific is very similar to the density structure observed on the same section. The similarity in the transient tracer distributions shown in Figure 4 is an indication of the strong control that transport plays in the ocean storage of these tracers. The differences between the tracers, particularly in the shallow waters, reflect the different equilibration times (~10 years for bomb C-14, ~1 year for anthropogenic CO_2, and weeks for pCFC) and the differing atmospheric histories.

[33] The relatively shallow penetration of anthropogenic CO_2 in the North Pacific is in strong contrast to the Atlantic distribution where anthropogenic CO_2 has penetrated all the

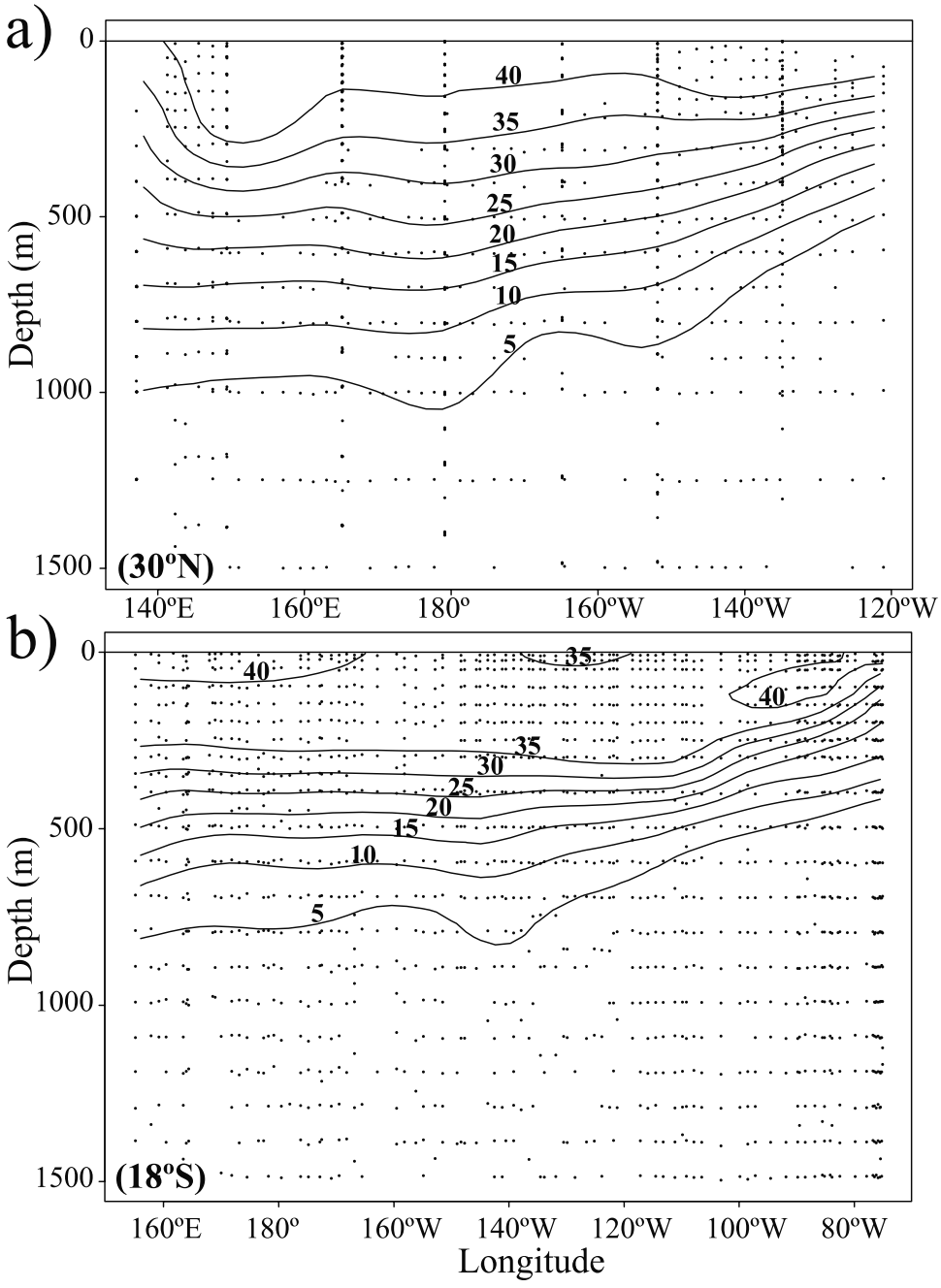

Figure 5. Zonal sections of anthropogenic CO_2 in μmol kg^{-1} along (a) WOCE line P2 at 30°N and (b) line P21 at 18°S. Points indicate sample locations.

way to the bottom in the northern high latitudes [*Gruber et al.*, 1996; *Wanninkhof et al.*, 1999; *Körtzinger et al.*, 1999]. These differences result from the lack of any significant deep water formation in the North Pacific [*Reid*, 1997] and the long timescales for replacement of North Pacific deep waters from the south [*Stuiver et al.*, 1983]. In the North Pacific, deep ventilation within the Kuroshio Extension and the subsequent circulation in the subtropical gyre generates a strong zonal gradient in the anthropogenic CO_2 penetration depth (Figure 5a). At approximately 30°N (WOCE line P2), the 5 μmol kg^{-1} contour is found at a depth of about 500 m near the North American coast, but deepens to approximately 1000 m off Japan. Likewise, the density structure imposed by the large-scale circulation and Ekman pumping in the subtropical gyre generates a zonal gradient in the South Pacific (Figure 5b). The isolines at approximately 18°S (WOCE line P21) get progressively deeper from east to west over approximately 60° of longitude. West of ~140°W the isolines are relatively flat. The broad scale of this eastern feature is related to the broad, slow nature of the currents in the gyre interior (in this case the South Equatorial Current). This is in contrast to the narrowly

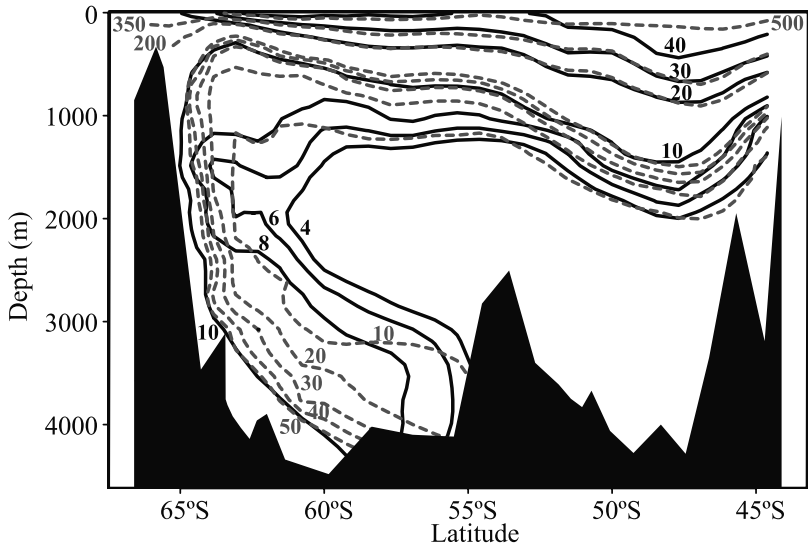

Figure 6. Meridional section of anthropogenic CO_2 in μmol kg^{-1} (solid contours) and pCFC-12 in patm (dashed contours) along WOCE line SR3 at 145°E. Black areas indicate ocean bottom.

focused western boundary currents, which are not clearly resolved in the smoothed maps of these sections. The longitudinal scale of the deepening isolines in the eastern basins is similar in both the North and South Pacific (Figure 5). The differences in penetration depths between the two sections are related to the location of the sections within the bowl-shaped subtropical gyres. The deepest penetrations are found in the South Pacific (Figure 4b), but the penetration depths along P21 were generally shallower than along P2 because the former cruise was run at a lower latitude (18°S) than P2 (30°N). Thus, P21 was farther from the deepest part of its subtropical gyre than P2.

[34] One feature that has been noted by numerous investigators over the years is the very shallow penetration of anthropogenic CO_2 in the high-latitude Southern Ocean [e.g., *Chen*, 1982b; *Poisson and Chen*, 1987; *Caldeira and Duffy*, 2000]. This same feature was observed with the ΔC* estimates in the Indian Ocean [*Sabine et al.*, 1999] and the Atlantic [*Gruber*, 1998], although the Southern Ocean data used for the Atlantic analysis were very sparse. Very shallow anthropogenic CO_2 penetration is also generally observed in the Pacific sector of the high-latitude Southern Ocean. One exception to this is found in the far southwestern Pacific where there is evidence of anthropogenic CO_2 in the northward moving bottom waters. This can be seen most clearly in the SR3 section (145°E) south of Tasmania (Figure 6). Bottom water concentrations as high as 10 μmol kg^{-1} are seen near the coast at the southern end

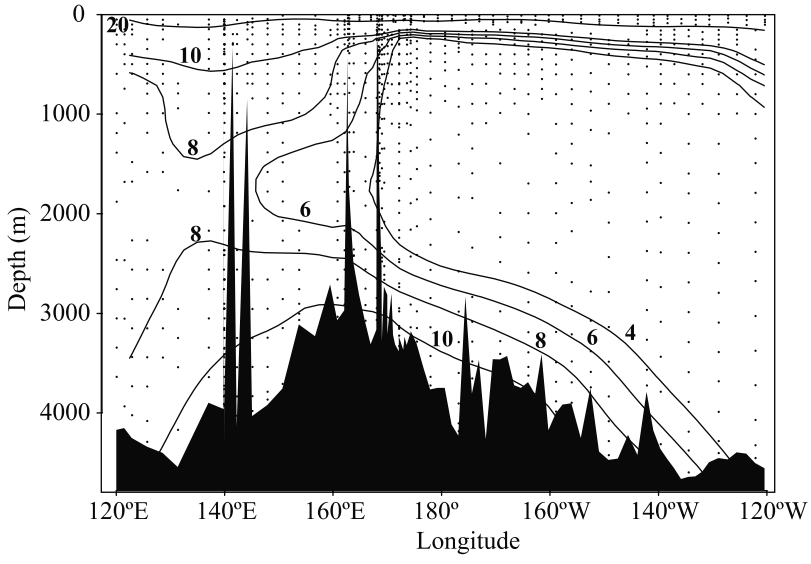

Figure 7. Zonal section of anthropogenic CO_2 in μmol kg^{-1} along WOCE line S4 at 62–67°S. Points indicate sample locations. Black areas indicate ocean bottom.

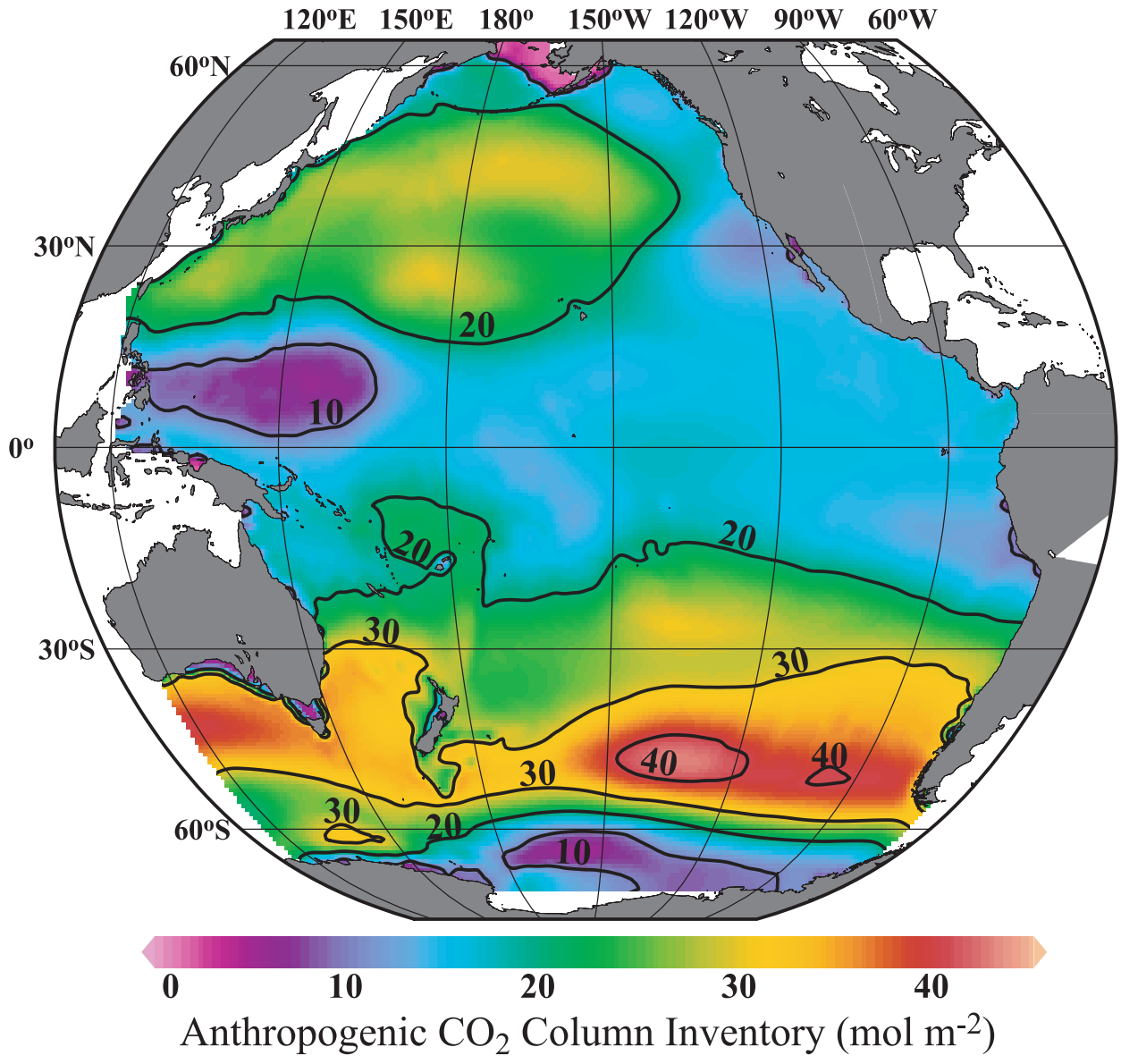

Figure 8. Map of anthropogenic CO_2 column inventory (mol m^{-2}) in the Pacific.

of the section. The bottom waters observed on this section are likely to be newly formed bottom water from the Adelie Land coast [*Rintoul*, 1998; *Rintoul and Bullister*, 1999]. These waters also have relatively high concentrations of CFCs, so one might expect to find anthropogenic CO_2 in these waters. Although the concentrations of anthropogenic CO_2 are very near the estimated detection limit of ~5 μmol kg^{-1} and there are serious uncertainties associated with incomplete equilibration of gases and cross-isopycnal mixing at high latitudes, the pCFC-12 distribution correlates well with the anthropogenic CO_2 distributions. Results from the zonal S4 lines, at 62–67°S, suggest that measurable anthropogenic CO_2 concentrations may extend as far east as 130°W–140°W at this latitude (Figure 7). The waters east of the date line do not have measurable concentrations of anthropogenic CO_2 in the central water column, between 500 and 2500 m. The bottom waters observed at these longitudes are presumably forming further to the south, in the Ross Sea.

[35] The basin-wide distribution of anthropogenic CO_2 can be summarized with a map of the anthropogenic CO_2 column inventory (Figure 8). The highest inventories are generally observed in the South Pacific between 45°S and 55°S. High column inventories are also observed off the Adelie coast of Antarctica at approximately 140°E. Aside from this region, where bottom water formation distributes anthropogenic CO_2 throughout the water column, the high-latitude Southern Ocean has generally low column inventories. There is also a relative minimum in inventory in the tropics because of shallow penetration at these latitudes. The North Pacific inventory maximum has lower inventories than the South Pacific and is shifted toward the west. The strong zonal inventory gradient in the North Pacific most likely results from deeper ventilation of the western

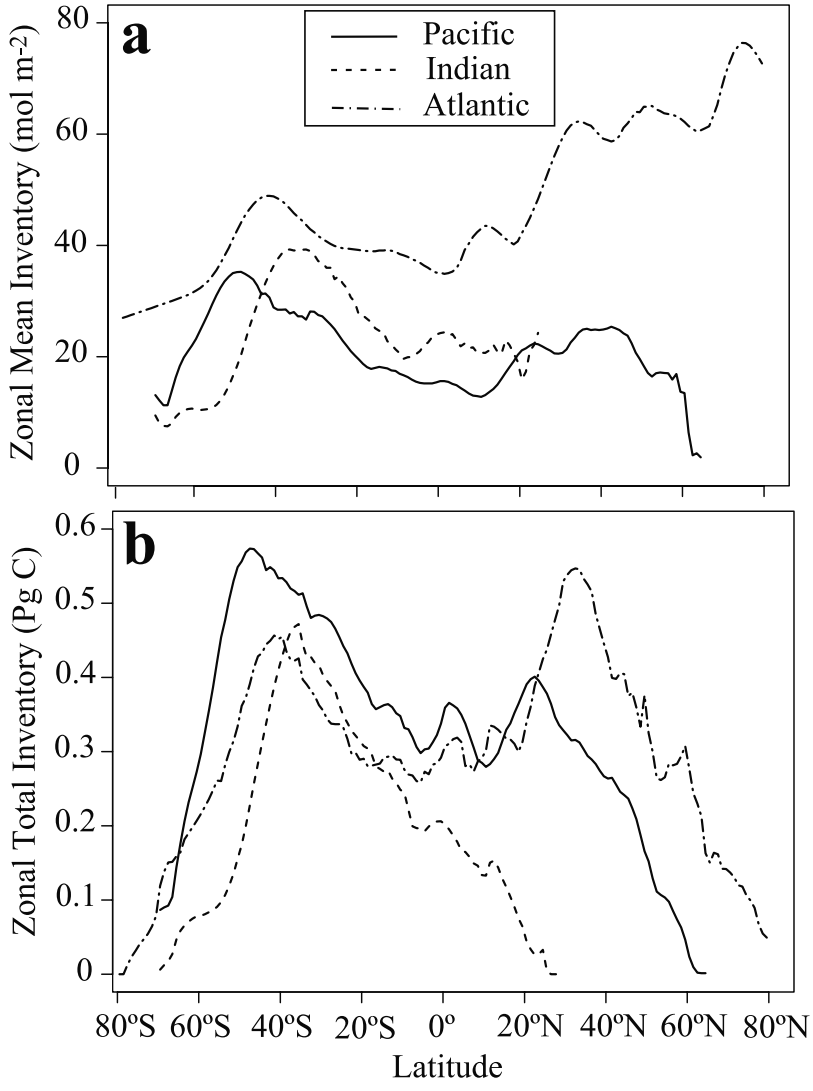

Figure 9. Plots of (a) zonal mean inventory in mol m^{-2} and (b) zonal total inventory Pg C for the Pacific, Indian, and Atlantic oceans versus latitude. Indian values are from *Sabine et al.* [1999]. Atlantic values are from *Gruber* [1998].

waters and the transport of anthropogenic CO_2 into the thermocline associated with the formation of North Pacific Intermediate Waters in the Sea of Okhotsk [*Warner et al.*, 1996]. The total inventory for the shaded region in Figure 8 is 44.5 ± 5 Pg C for a mean year of 1994. Approximately 28 Pg C is located in the Southern Hemisphere and 16.5 Pg C is located north of the equator.

6. Comparison With Other Oceans

[36] The Southern Hemispheric distributions of anthropogenic CO_2 look similar in the Atlantic, Indian, and Pacific Oceans. The penetration depth (estimated from the depth of the 5 μmol kg^{-1} contour) was estimated by *Gruber* [1998] to be close to 2000 m in the Subtropical Convergence region of the South Atlantic. The Indian and Pacific penetrations are closer to ~1300 m in this region (e.g., Figure 4b). It is unknown at this time whether this difference is real or reflects small differences in the data, technique, or gridding methods. There are also differences in the location of the maximum penetration and largest column inventories of the three different basins. Figure 9 compares the zonal mean inventory and the zonal total inventory for the Pacific, Indian, and Atlantic oceans [*Sabine et al.*, 1999; *Gruber*, 1998]. The maximum in zonal mean inventory in the Indian Ocean is at 35–40°S, approximately 15° north of the South Pacific maximum. These differences and the location of the column inventory maximum observed in Figure 8 are consistent with known zonal variations in the location of the Subtropical Convergence. The Pacific has the largest total inventory in all of the southern latitudes (Figure 9b) despite the fact that it generally has the lowest average inventory when normalized to a unit area (Figure 9a).

[37] In the higher northern latitudes the area-specific inventories of the Atlantic can be three times higher than in the Pacific because of the formation of North Atlantic Deep waters that transport anthropogenic CO_2 into the

ocean interior. These large values are sufficient to make total inventories highest in the Atlantic despite the larger area of the Pacific. One should also note that the Atlantic values of *Gruber* [1998] represent inventories from the late 1980s. These values would be somewhat higher if they were scaled up to the WOCE timeframe. Deeper anthropogenic CO_2 penetration was observed on the western side of the North Atlantic by *Gruber et al.* [1996], but the zonal gradient was much more localized to the western basin than observed in the North Pacific. These differences primarily result from differences in the deep circulation in the two oceans.

7. Comparison With Models

[38] Since the exact distribution of anthropogenic CO_2 cannot be directly measured, it is useful to compare estimates derived from different approaches. Recently *Xu et al.* [2000] examined the uptake and storage of anthropogenic CO_2 with a medium resolution ($2^\circ \times 2^\circ \times 28$ levels) basin-wide OGCM of the North Pacific. This study examined the impact of changing the isopycnal diffusivity on the anthropogenic uptake of the model. Although all of the model runs presented by *Xu et al.* [2000] estimated higher North Pacific inventories (19.4–22.01 Pg C north of equator) than determined with this study (16.5 Pg C north of equator), the model run with the lowest diffusivities gave results that were most consistent with the estimates presented here. Thus, observational based estimates, such as these, can provide a useful diagnostic tool for evaluating models.

[39] Likewise, models can help evaluate various observational based approaches. For example, *Xu et al.* [2000] also compared their results in the western North Pacific with the results of *Chen* [1993a]. They noted that Chen had a deeper penetration and stronger meridional changes in penetration depth than could be generated with the model. Our results, however, are much more similar to the model distributions with penetration depths close to 1000 m and meridional changes in penetration depth about half (250 m) of that observed by *Chen* [1993a] in the western North Pacific.

[40] Moreover, models can also provide a link between the observational based inventory estimates and anthropogenic CO_2 uptake from the atmosphere. Interestingly, the *Xu et al.* [2000] model run with distributions most similar to our results also had the largest uptake of anthropogenic CO_2 in the equatorial region. All model runs indicated that the equatorial Pacific had a very large uptake of anthropogenic CO_2 but, as *Xu et al.* [2000] noted, large fluxes do not imply large inventories because most of that carbon is transported into the subtropical gyres. Most of the equatorial anthropogenic CO_2 uptake in the model, however, was transported to the south, an area where the model inventories were substantially larger than the inventories estimated here. More work is needed to understand the implications of these differences.

[41] A formal comparison of the results presented here, as well as ΔC^* based estimates for the Indian and Atlantic Oceans, is being conducted with the 13 global ocean carbon models affiliated with the international ocean carbon model intercomparison project (OCMIP-2). Preliminary results indicate that our Pacific inventory estimates fall within the range of model estimates. The anthropogenic carbon distributions, however, varied greatly between the data and different models. The largest differences, both between the data based estimates and between the different models, were found in the Southern Ocean. This is similar to the findings of the first OCMIP exercise [*Orr et al.*, 2001]. Generally, the models that had much higher Southern Ocean anthropogenic CO_2 inventories relative to the observations were the same models that overestimated the CFC inventories [*Dutay et al.*, 2002]. A manuscript detailing the comparison and implications for the improvement of both model and observation based estimates is in preparation.

8. Conclusions

[42] The ΔC^* approach for estimating anthropogenic CO_2 has been applied now in the three major oceans: the Atlantic, Indian, and Pacific. Small modifications to the technique continue to improve the quality of the results. Each time the technique is applied to a new region, new challenges are faced. We believe the addition of the OMP analysis in this work has greatly improved the anthropogenic estimates by explicitly accounting for the mixing of different water types. The basic principles of the technique, however, have remained the same and appear to be sound. Many of the general features observed in this work are consistent with trends observed in the other basins: high column inventories and relatively deep penetrations associated with the Subtropical Convergence zones, relatively low inventories in the equatorial and high-latitude Southern Ocean regions, and deep penetration of anthropogenic CO_2 in areas of deep and bottom water formation.

[43] The total Pacific anthropogenic CO_2 inventory (44.5 $\pm$ 5 Pg C in 1994) is relatively low compared to the area of this ocean. This relatively low inventory primarily results from large-scale circulation within the Pacific. The deep waters of the Pacific are among the oldest in the global oceans and thus have not been exposed to anthropogenic contamination. The lack of deep-water formation in the North Pacific results in relatively little penetration of anthropogenic CO_2 into the ocean interior. The tremendous area, diversity of habitats, and corrosiveness of the Pacific waters with respect to carbonate minerals, however, provide the potential for significant changes in carbon cycling in this ocean as a result of future climate change. Some of these changes may lead to changes in the role of the Pacific as a sink for anthropogenic CO_2. The global CO_2 survey data and estimates provided here make an important baseline for assessing future changes in the Pacific carbon cycle.

[44] **Acknowledgments.** We wish to thank all of those who contributed to the Pacific data set compiled for this project, including those responsible for the carbon measurements and the CFC measurements, and the Chief Scientists. The amount of work that went into collecting, finalizing, and synthesizing these data in a manner that makes a publication like this possible can never be properly acknowledged. We also acknowledge the helpful comments of A. Dickson and an anonymous reviewer. This work was funded by NASA grant NAG5-6591, NOAA/DOE grant GC99-220, and the Joint Institute for the Study of the Atmosphere and Ocean (JISAO) under NOAA Cooperative Agreement NA67RJ0155, JISAO Contribution 863, and PMEL contribution 2378. We thank Lisa Dilling

of the NOAA Office of Global Programs and Donald Rice of the National Science Foundation for their efforts in the coordination of this study.

References

Anderson, L. A., On the hydrogen and oxygen content of marine phytoplankton, *Deep Sea Res., Part I*, *42*, 1675–1680, 1995.

Anderson, L. A., and J. L. Sarmiento, Redfield ratios of remineralization determined by nutrient data analysis, *Global Biogeochem. Cycles*, *8*, 65–80, 1994.

Bradshaw, A. L., P. G. Brewer, D. K. Shafer, and R. T. Williams, Measurements of total carbon dioxide and alkalinity by potentiometric titration in the GEOSECS program, *Earth Planet. Sci. Lett.*, *55*, 99–115, 1981.

Brewer, P. G., Direct observation of the oceanic CO_2 increase, *Geophys. Res. Lett.*, *5*, 997–1000, 1978.

Brewer, P. G., C. Goyet, and G. Friederich, Direct observation of the oceanic CO_2 increase revisited, *Proc. Natl. Acad. Sci.*, *94*, 8308–8313, 1997.

Broecker, W. S., "NO," a conservative water-mass tracer, *Earth Planet. Sci. Lett.*, *23*, 100–107, 1974.

Broecker, W. S., and T.-H. Peng, Gas exchange rates between air and sea, *Tellus*, *26*, 21–35, 1974.

Broecker, W. S., D. W. Spencer, and H. Craig, *GEOSECS Pacific Expedition*, vol. 3, Hydrographic Data 1973–1974, 137 pp., Natl. Sci. Found., U.S. Gov. Print. Off., Washington, D. C., 1982.

Broecker, W. S., T. Takahashi, and T.-H. Peng, Reconstruction of past atmospheric CO_2 contents from the chemistry of the contemporary ocean: An evaluation, *TR020, DOE/OR-857*, 79 pp., U.S. Dep. of Energy, Washington, D. C., 1985.

Caldeira, K., and P. B. Duffy, The role of the Southern Ocean in uptake and storage of anthropogenic carbon dioxide, *Science*, *287*, 620–622, 2000.

Carbon Dioxide Information Analysis Center, *Trends Online: A Compendium of Data on Global Change*, Oak Ridge Natl. Lab., U.S. Dep. of Energy, Oak Ridge, Tenn., 2001. (Available at http://cdiac.esd.ornl.gov/trends/trends.htm)

Chen, C.-T. A., Oceanic penetration of excess CO_2 in a cross section between Alaska and Hawaii, *Geophys. Res. Lett.*, *9*, 117–119, 1982a.

Chen, C.-T. A., On the distribution of anthropogenic CO_2 in the Atlantic and Southern Oceans, *Deep Sea Res.*, *29*, 563–580, 1982b.

Chen, C.-T. A., On the depth of anthropogenic CO_2 penetration in the Atlantic and Pacific Oceans, *Oceanol. Acta*, 97–102, No. sp., 1987.

Chen, C.-T. A., Anthropogenic CO_2 distribution in the North Pacific Ocean, *J. Oceanogr.*, *49*, 257–270, 1993a.

Chen, C.-T. A., The oceanic anthropogenic CO_2 sink, *Chemosphere*, *27*(6), 1041–1064, 1993b.

Chen, C.-T. A., and F. J. Millero, Gradual increase of oceanic CO_2, *Nature*, *277*, 205–206, 1979.

Coatanoan, C., C. Goyet, N. Gruber, C. L. Sabine, and M. Warner, Comparison of two approaches to quantify anthropogenic CO_2 in the ocean: Results from the northern Indian Ocean, *Global Biogeochem. Cycles*, *15*, 11–25, 2001.

Deutsch, C., N. Gruber, R. M. Key, J. L. Sarmiento, and A. Ganachaud, Denitrification and N_2 fixation in the Pacific Ocean, *Global Biogeochem. Cycles*, *15*, 483–506, 2001.

Dickson, A. G., and F. J. Millero, A comparison of the equilibrium constants for the dissociation of carbonic acid in seawater media, *Deep Sea Res.*, *34*, 1733–1743, 1987.

Dickson, A. G., G. C. Anderson, and J. D. Afghan, Sea water based reference materials for CO_2 analysis, 1, Preparation, distribution and use, *Mar. Chem.*, in press, 2002a.

Dickson, A. G., J. D. Afghan, and G. C. Anderson, Sea water reference materials for CO_2 analysis, 2, A method for the certification of total alkalinity, *Mar. Chem.*, in press, 2002b.

Dutay, J.-C., et al., Evaluation of ocean model ventilation with CFC-11: Comparison of 13 global ocean models, *Ocean Modell. 4*, pp. 89–120, Hooke Inst., Oxford Univ., Oxford, England, 2002.

Feely, R. A., R. Wanninkhof, T. Takahashi, and P. Tans, Influence of El Niño on the equatorial Pacific contribution to atmospheric CO_2 accumulation, *Nature*, *398*, 597–601, 1999a.

Feely, R. A., C. L. Sabine, R. M. Key, and T.-H. Peng, CO_2 survey synthesis results: Estimating the anthropogenic carbon dioxide sink in the Pacific Ocean, *U. S. JGOFS News*, *9*(4), 1–4, 1999b.

Goyet, C., and D. Davis, Estimation of total CO_2 concentration throughout the water column, *Deep Sea Res., Part I*, *44*, 859–877, 1997.

Goyet, C., C. Coatanoan, G. Eischeid, T. Amaoka, K. Okuda, R. Healy, and S. Tsunogai, Spatial variation of total CO_2 and total alkalinity in the northern Indian Ocean: A novel approach for the quantification of anthropogenic CO_2 in seawater, *J. Mar. Res.*, *57*, 135–163, 1999.

Gruber, N., Anthropogenic CO_2 in the Atlantic Ocean, *Global Biogeochem. Cycles*, *12*, 165–191, 1998.

Gruber, N., and J. L. Sarmiento, Global patterns of marine nitrogen fixation and denitrification, *Global Biogeochem. Cycles*, *11*, 235–266, 1997.

Gruber, N., J. L. Sarmiento, and T. F. Stocker, An improved method for detecting anthropogenic CO_2 in the oceans, *Global Biogeochem. Cycles*, *10*, 809–837, 1996.

Holfort, J., K. M. Johnson, B. Schneider, G. Siedler, and D. W. R. Wallace, Meridional transport of dissolved inorganic carbon in the South Atlantic Ocean, *Global Biogeochem. Cycles*, *12*, 479–499, 1998.

Inoue, H. Y., H. Matsueda, M. Ishii, K. Fushimi, M. Hirota, I. Asanuma, and Y. Takasugi, Long-term trend of the partial pressure of carbon dioxide (pCO_2) in surface waters of the western North Pacific, 1984–1993, *Tellus, Ser. B*, *47*, 391–413, 1995.

Johnson, G. C., P. E. Robbins, and G. E. Hufford, Systematic adjustments of hydrographic sections for internal consistency, *J. Atmos. Oceanic Technol.*, *18*, 1234–1244, 2001.

Karstensen, J., and M. Tomczak, Age determination of mixed water masses using CFC and oxygen data, *J. Geophys. Res.*, *103*, 18,599–18,610, 1998.

Keeling, C. D., and T. P. Whorf, Atmospheric CO_2 records from sites in the SIO air sampling network, in *Trends: A Compendium of Data on Global Change*, Carbon Dioxide Info. Anal. Cent., Oak Ridge Natl. Lab., U.S. Dep. of Energy, Oak Ridge, Tenn., 2000.

Körtzinger, A., M. Rhein, and L. Mintrop, Anthropogenic CO_2 and CFCs in the North Atlantic Ocean—A comparison of man-made tracers, *Geophys. Res. Lett.*, *26*, 2065–2068, 1999.

Krumgalz, B. S., J. Erez, and C.-T. A. Chen, Anthropogenic CO_2 penetration in the northern Red Sea and in the Gulf of Elat (Aqaba), *Oceanol. Acta*, *13*(3), 283–290, 1990.

Lamb, M. F., et al., Consistency and synthesis of Pacific Ocean CO_2 survey data, *Deep Sea Res., Part II*, *49*, 21–58, 2002.

Merhbach, C., C. H. Culberson, J. E. Hawley, and R. M. Pytkowicz, Measurement of the apparent dissociation constants of carbonic acid in seawater at atmospheric pressure, *Limnol. Oceanogr.*, *18*, 897–907, 1973.

Ono, T., S. Watanabe, K. Okuda, and M. Fukasawa, Distribution of total carbonate and related properties in the North Pacific along 30°N, *J. Geophys. Res.*, *103*, 30,873–30,883, 1998.

Ono, T., Y. W. Watanabe, and S. Watanabe, Recent increase of DIC in the western North Pacific, *Mar. Chem.*, *72*, 317–328, 2000.

Orr, J. C., et al., Global oceanic uptake of anthropogenic carbon dioxide as predicted by four 3-D ocean models, *Global Biogeochem. Cycles*, *15*, 43–60, 2001.

Papaud, A., and A. Poisson, Distribution of dissolved CO_2 in the Red Sea and correlation with other geochemical tracers, *J. Mar. Res.*, *44*, 385–402, 1986.

Pérez, F. F., L. Mintrop, O. Llinás, M. Glez-Dávila, C. G. Castro, M. Alvarez, A. Körtzinger, M. Santana-Casiano, M. J. Rueda, and A. F. Ríos, Mixing analysis of nutrients, oxygen and inorganic carbon in the Canary Islands region, *J. Mar. Syst.*, *28*, 183–201, 2001.

Poisson, A., and C.-T. A. Chen, Why is there little anthropogenic CO_2 in the Antarctic Bottom Water?, *Deep Sea Res., Part A*, *34*, 1255–1275, 1987.

Quay, P. D., B. Tilbrook, and C. S. Wong, Oceanic uptake of fossil fuel CO_2: Carbon-13 evidence, *Science*, *256*, 74–79, 1992.

Reid, J. L., On the total geostrophic circulation of the Pacific Ocean: Flow patterns, tracers, and transports, *Prog. Oceanogr.*, *39*, 263–352, 1997.

Rintoul, S. R., On the origin and influence of Adelie Land Bottom Water, in *Ocean, Ice, and Atmosphere: Interactions at the Continental Margin, Antarct. Res. Ser: Phys. Sci.*, vol. 75, edited by S. S. Jacobs and R. F. Weiss, pp. 151–171, AGU, Washington, D. C., 1998.

Rintoul, S. R., and J. L. Bullister, A late winter hydrographic section from Tasmania to Antarctica, *Deep Sea Res.*, *46*, 1417–1454, 1999.

Rubin, S., and R. M. Key, Separating natural and bomb-produced radiocarbon in the ocean: The potential alkalinity method, *Global Biogeochem. Cycles*, doi:10.1029/2001GB001432, in press, 2002.

Sabine, C. L., and R. A. Feely, Comparison of recent Indian Ocean anthropogenic CO_2 estimates with a historical approach, *Global Biogeochem. Cycles*, *15*, 31–42, 2001.

Sabine, C. L., R. M. Key, K. M. Johnson, F. J. Millero, A. Poisson, J. L. Sarmiento, D. W. R. Wallace, and C. D. Winn, Anthropogenic CO_2 inventory of the Indian Ocean, *Global Biogeochem. Cycles*, *13*, 179–198, 1999.

Sambrotto, R. N., G. Savidge, C. Robinson, P. Boyd, T. Takahashi, D. M. Karl, C. Langdon, D. Chipman, J. Marra, and L. Codispoti, Elevated consumption of carbon relative to nitrogen in the surface ocean, *Nature*, *363*, 248–250, 1993.

Sarmiento, J. L., J. Willebrand, and S. Hellerman, Objective analysis of tritium observations in the Atlantic Ocean during 1971–74, *Tech Rep. 1*, 19 pp., Ocean Tracers Lab., Princeton Univ., Princeton, N. J., July 1982.

Shiller, A. M., Calculating the oceanic CO_2 increase: A need for caution, *J. Geophys. Res.*, *86*, 11,083–11,088, 1981.

Slansky, C. M., R. A. Feely, and R. Wanninkhof, The stepwise linear regression method for calculating anthropogenic CO_2 invasion into the North Pacific Ocean, in *Biogeochemical Processes in the North Pacific: Proceedings of the International Marine Science Symposium*, edited by S. Tsunogai, pp. 70–79, Jap. Mar. Sci. Found., Tokyo, 1997.

Stuiver, M., P. D. Quay, and H. G. Ostlund, Abyssal water carbon-14 distribution and the age of the world oceans, *Science*, *219*, 849–851, 1983.

Takahashi, T., R. H. Wanninkhof, R. A. Feely, R. F. Weiss, D. W. Chipman, N. Bates, J. Olafsson, C. Sabine and S. C. Sutherland, Net air-sea CO_2 flux over global oceans: An improved estimate based on sea-air pCO_2 difference, in *Proceedings of 2nd International Symposium on CO_2 in the Oceans, CGER-IO37-99*, pp. 9–15, CGER/NIES, Tsukuba, Japan, 1999.

Tomczak, M., A multi-parameter extension of temperature/salinity diagram techniques for the analysis of non-isopycnal mixing, *Prog. Oceanogr.*, *10*, 147–171, 1981.

Tomczak, M., and D. G. B. Large, Optimum multiparameter analysis of mixing in the thermocline of the eastern Indian Ocean, *J. Geophys. Res.*, *94*, 16,141–16,149, 1989.

Tsunogai, S., T. Ono, and S. Watanabe, Increase in total carbonate in the western North Pacific water and a hypothesis on the missing sink of anthropogenic carbon, *J. Oceanogr.*, *49*, 305–315, 1993.

Wallace, D. W. R., Storage and transport of excess CO_2 in the oceans: The JGOFS/WOCE Global CO_2 Survey, in *Ocean Circulation and Climate: Observing and Modelling the Global Ocean*, edited by G. Siedler, J. Church, and J. Gould, pp. 489–521, Academic, San Diego, Calif., 2001.

Wanninkhof, R., S. C. Doney, T.-H. Peng, J. L. Bullister, K. Lee, and R. A. Feely, Comparison of methods to determine the anthropogenic CO_2 invasion into the Atlantic Ocean, *Tellus, Ser. B*, *51*, 511–530, 1999.

Warner, M. J., J. L. Bullister, D. P. Wisegarver, R. H. Gammon, and R. F. Weiss, Basin-wide distributions of chlorofluorocarbons CFC-11 and CFC-12 in the North Pacific: 1985–1989, *J. Geophys. Res.*, *101*, 20,525–20,542, 1996.

Watanabe, Y. W., T. Ono, and A. Shimamoto, Increase in the uptake rate of oceanic anthropogenic carbon in the North Pacific determined by CFC ages, *Mar. Chem.*, *72*, 297–315, 2000.

Winn, C. D., Y.-H. Li, F. T. Mackenzie, and D. M. Karl, Rising surface ocean dissolved inorganic carbon at the Hawaii Ocean Time-series site, *Mar. Chem.*, *60*, 33–47, 1998.

Xu, Y., Y. W. Watanabe, S. Aoki, and K. Harada, Simulations of storage of anthropogenic carbon dioxide in the North Pacific using an ocean general circulation model, *Mar. Chem.*, *72*, 221–238, 2000.

You, Y., and M. Tomczak, Thermocline circulation and ventilation in the Indian Ocean derived from water mass analysis, *Deep Sea Res.*, *40*, 13–56, 1993.

J. L. Bullister and R. A. Feely, NOAA/Pacific Marine Environmental Laboratory, 7600 Sand Point Way NE, Seattle, WA 98115, USA. (bullister@pmel.noaa.gov; feely@pmel.noaa.gov)

R. M. Key, AOS Program, Princeton University, Forrestal Campus/Sayre Hall, Princeton, NJ 08544, USA. (key@princeton.edu)

K. Lee, School of Environmental Science and Engineering, Pohang University of Science and Technology, San 31, Nam-gu, Hyoja-dong, Pohang, 790-784, Republic of Korea. (ktl@postech.ac.kr)

F. J. Millero, University of Miami/RSMAS, 4600 Rickenbacker Causeway, Miami, FL 33149, USA. (fmillero@rsmas.miami.edu)

T. Ono, Ecosystem Change Research Program, FRSGC/IGCR, 3173-25 Showa-machi, Kanazawa-ku, Yokohama 236-0001, Japan. (onot@frontier.esto.or.jp)

T.-H. Peng, NOAA/Atlantic Oceanographic and Meteorological Laboratory, 4301 Rickenbacker Causeway, Miami, FL 33149, USA. (peng@aoml.noaa.gov)

C. L. Sabine, Joint Institute for the Study of Atmosphere and Ocean, University of Washington, c/o NOAA/PMEL, 7600 Sand Point Way NE, Seattle, WA 98115, USA. (sabine@pmel.noaa.gov)

B. Tilbrook, CSIRO, Division of Oceanography, GPO Box 1538, Hobart, Tasmania 7001, Australia.

C. S. Wong, Institute of Ocean Sciences, 9860 West Saanich Road, Sidney, British Columbia V8L 4B2, Canada. (wongc@dfo-mpo.gc.ca)